This article has been published in Metallurgical and Materials Transactions A. The final publication is available at Springer via https://doi.org/10.1007/s11661-017-4097-7

A combined numerical-experimental approach to quantify the thermal contraction of A356 during solidification

J.P. Macht[1], D.M. Maijer[1], A.B. Phillion[2]
Corresponding Author: andre.phillion@mcmaster.ca

[1] Department of Materials Engineering, The University of British Columbia, Vancouver, Canada, V6T 1Z4
[2] Department of Materials Science and Engineering, McMaster University, Hamilton, Canada, L8S 4L7

Abstract

A process for generating thermal contraction coefficients for use in the solidification modelling of aluminum castings is presented. Sequentially-coupled thermal stress modelling is used in conjunction with experimentation to empirically generate the thermal contraction coefficients for a strontium modified A356 alloy. The impact of cooling curve analysis on the modelling procedure is studied. Model results are in good agreement with experimental findings, indicating a sound methodology for quantifying the thermal contraction. The technique can be applied to other commercially relevant aluminum alloys, increasing the utility of solidification modelling in the casting industry.

Introduction

The coefficient of thermal expansion strongly influences the geometry and residual stress in as-cast aluminum components, and must be considered as part of the design process. In fully solid materials, temperature changes manifest as variations in material density, resulting in thermal strains that can lead to thermal stresses when a component is constrained. These thermal strains are commonly measured via dilatometry. In semi-solid materials, the situation is more complex. On one hand, the transition from liquid to solid induces a significant density difference, resulting in large solidification contraction as compared to the expected thermal contraction of the solid phases. On the other hand, liquid feeding, shrinkage porosity, and plastic deformation of the solid phase partially negate some of the effects resulting from solidification contraction. This results in complex, large (relative to single-phase thermal expansion/contraction), and non-linear contraction behavior that occurs throughout the solidification regime [1]. Note that in this article we define the term solidification contraction to represent the thermal contraction occurring within the semi-solid temperature range. Further, we define the term rigidity point as the fraction solid at which a continuous dendritic network is formed, and the material starts to develop strength. When the fraction solid is above the rigidity point, the solidification contraction of the solid at the microstructural level can cause geometric distortions, and residual stresses at the component level. However, when the fraction solid is below the rigidity point, the solidification contraction is mostly compensated by fluid flow.

Eskin et al. developed an experimental technique based on an idea proposed by Novikov [2] to measure linear solidification contraction [3]. The apparatus consists of a T-shaped graphite mould that is placed on a water-cooled copper chill, and a moving wall at the base that is connected to a linear-voltage displacement sensor (LVDT). The T-shaped geometry ensures that the horizontal arms restrain the rest of the casting. The displacement of the moving wall as a function of temperature within this casting is measured during each experiment. Eskin et al. used the LVDT data to calculate a temperature-dependent thermal contraction coefficient (TCC) at high sub-solidus temperatures,

$$TCC = \frac{\Delta L/L_{gauge}}{\Delta T} \quad \text{(Eq.1)}$$

where ΔT represents the change in temperature for a given time increment at a position in the casting near the moving wall, ΔL represents the change in position of the displacement sensor for the same time increment, and L_{gauge} is the initial length of the sample. This apparatus was used to test a number of wrought aluminum alloys as well as steels, demonstrating a positive correlation between the magnitude of solidification contraction and the occurrence of hot tearing.

Finite Element Analysis (FEA) is routinely used to model industrial casting processes. Heat transfer, fluid flow, and stresses can all be simulated to understand material behavior and defect formation. To accurately model stress development, knowledge of the thermal contraction behavior occurring during solidification is key. However, because of its highly non-linear behavior, solidification contraction is challenging to quantify consistently and its study requires a multi-faceted approach. The approach used by Eskin to measure linear solidification contraction [3] is useful for obtaining the required experimental data. However, because of strong thermal gradients within a casting, Eq. 1 provides only an estimate of the solidification contraction, and not quantified solidification contraction coefficients that can be used for modelling purposes.

In this research, a combined experimental/numerical method is presented to quantify the thermal strains and the corresponding solidification contraction coefficients experienced by aluminum alloys. The Al-Si casting alloy A356 is used as the exemplar system. First, small ingots are cast following a method similar to Eskin's approach to measure solidification contraction. Second, thermal-stress numerical modeling is used to quantify the heat transfer and thermal contraction behavior during solidification; the input solidification contraction coefficients are adjusted in successive model iterations until the overall linear contraction predicted by the model matches the experimentally-measured linear contraction. This new coupled methodology provides insight into high-temperature solidification contraction of metals, and can be easily applied to other systems in order to quantify the solidification contraction coefficients required for predicting hot tearing in macro-scale casting models.

Experimental

Materials: The material used in this study was strontium-modified A356 (Al – 7 wt% Si, 0.3 wt% Mg, 0.003 wt% Na, 0.008 wt% Sr). This Al-Si foundry alloy is prevalent in the automotive industry due to its good castability and good mechanical properties that can be obtained through heat treatment [4]. Strontium modification is employed to alter the morphology of the Si precipitate from a blocky structure to an interconnected fibrous phase [5].

Apparatus Design: The experimental setup used to measure the linear contraction is based on the T-shape design of Eskin et al. mentioned in the Introduction. An image of the experimental apparatus, along with the dimensions of the mold and an image of the sample itself are given in Figure 1. Note that while Eskin [3] placed the water-cooled copper chill below the graphite mold, it is placed at the head of the T-shape in this work.

The goal of these experiments is to measure the horizontal linear contraction. Moving the water-cooled copper chill to the head of the T-shape causes directional solidification in the horizontal direction, which then enables the horizontal contraction to be measured directly. Specifically, the horizontal linear contraction is measured by recording the displacement of a clearance-fit Invar rod that is embedded into the ingot through the moving wall at the base of the leg of the T-shape. The head of the T-shape provides a restraint that the leg of the T-shape contracts against. During casting, the melt solidifies and then contracts around one end of the rod while displacement is recorded using an LVDT (HR Series General Purpose LVDT configured with an ATA-2001

Analog LVDT/RVDT Signal Conditioner fabricated by Measurement Specialties Ltd.) mounted to the other end of the rod. It is important to note that contraction will also occur in the vertical direction of the casting because of heat transfer between the casting and the environment. Maintaining a truly unidirectional thermal gradient in the mold cavity and consequently unidirectional thermal contraction for the duration of the experiment is a challenging heat transfer requirement that is not met with this experimental methodology.

Understanding the temperature profile of the castings is essential to understanding the manner in which thermal stresses ultimately develop. For the temperature measurements, three type-K thermocouples are placed near the head (closest to the chill), center, and base (closest to the moving wall) of the T shape. These thermocouples were located at a height of ~12.5 mm below the open top of the mold.

Experimental Procedure: The experimental procedure consisted of first melting the A356 in a holding furnace, then pouring the melt into the graphite T-shaped mold at a casting temperature of 888 K (615˚C), and finally recording the displacement of the moving wall and the temperature evolution within the casting during solidification at a rate of 5 Hz until the center thermocouple reached 723 K (450˚C). Cold water was passed through the copper chill continuously at a flow rate of 20 L/min. In total, three experiments (Trials A, B, and C) were carried out using identical processing conditions. The average cooling rates measured during solidification for each experiment are listed in Table 1.

Numerical

Model Formulation: A 3D sequentially coupled thermal – stress model was developed within the Abaqus FEA software to simulate the evolution of temperature and stress/strain fields within the T-shaped casting during solidification and cooling to 723 K (450˚C). This model was applied to each of the three experiments. The term sequentially coupled implies that first the thermal field is calculated without consideration of the effects of stress, and then second the elastic stress analysis is performed using the nodal temperatures from the thermal analysis as a predefined field. The advantages of sequential coupling are twofold: (1) computational time is reduced and (2) multiple stress analyses with different material properties can be simulated for a given thermal analysis. The use of sequential coupling allowed for the decoupling of the objectives sought within each stage of the modelling procedure – tuning of the heat transfer coefficients in the thermal model and then quantifying the solidification contraction coefficients in the stress model.

Thermal Model

Geometry: The thermal model geometry consisted of one half of the T-shaped casting, as centerline symmetry was assumed (Figure 2a), as well as one-half of the graphite mold (Figure 2b).

Initial Conditions: The nodal temperatures of the casting and die were initially set to 888 K (615˚C) and 298 K (25˚C), respectively.

Boundary Conditions: To extract heat, a series of heat transfer coefficient boundary conditions were applied between the casting and/or mold and the surrounding environment. The values used to represent heat loss to the environment are given in Table 2, and were inferred from previous work [6]. These values were used for the thermal simulations of all three casting trials. The heat transfer across the interface between the casting and mold was modelled via a thermal contact conductance coefficient using the GAPCON user-written subroutine within the Abaqus FEA software. The temperature-dependent coefficients, given in Table 3, were tuned such that the predicted temperatures matched the experimental cooling curve collected at the center of the casting, TC2. This tuning process was performed on each thermal simulation in order to account for the observed differences in temperature evolution between the three casting trials. As can be seen in Table 3, the coefficients are slightly different between Trials A, B, and C. The fraction solid development and its inherent relationship to latent heat release was also incorporated into the model tuning process using the equation-based Newtonian (EBN) cooling curve analysis [7] developed by Gibbs and Mendez (the reason for and results of which are discussed later).

Material Properties: The thermo-physical (density, thermal conductivity, heat capacity and total latent heat) properties of A356 and graphite were based on values reported in the literature [4, 8].

Stress Model

Geometry: As friction between the mold and casting was assumed to be minimal, only one-half of the T-shape casting was included in the stress model.

Boundary Conditions: To provide mechanical restraint, it was assumed that the two surfaces of the T-shape providing the restraint remained in contact with the mold, (i.e. $u_x=u_y=u_z=0$ mm, where u is the displacement in the x, y, or z, directions) as shown in Figure 2. The base of the casting was also assumed to remain in contact with the mold ($u_z=0$).

Material Properties: The Young's modulus and Poisson's ratio of A356 and graphite were based on values reported in the literature [9, 10]. Following Hao et al. [11], it was assumed that the Young's modulus is only of significant magnitude at temperatures below the rigidity point, whereas above, it is only a small value. The rigidity point was assumed to occur at the temperature where the non-equilibrium primary eutectic reaction begins to occur, T_{Rigid} = 568˚C. The solidification contraction coefficients are the focus of this research and will be presented in the next section. The UEXPAN user-written subroutine was used in Abaqus to model the relevant thermal expansion behavior. The values were empirically determined via the tuning process such that one set of solidification contraction coefficients was used for the thermal-stress simulations of all three trials, while still producing accurate representations of the thermal contraction behavior seen in each experimental trial.

Results and Discussion

The evolution in temperature measured at TC2 during each casting experiment is shown in Figure 3a. As can be seen, the metal first underwent cooling in the liquid state, followed by primary solidification, then eutectic solidification, and finally solid state cooling. All three curves appear quite similar, demonstrating the repeatability of the methodology.

The thermocouple measurements TC1, TC2, and TC3 from Trial A are shown in Figure 3b along with the corresponding results from the numerical simulations. The cooling observed at these three locations is different due to their relative distance from the copper chill. Within the thermal model outlined in Section 3, the main adjustable parameter that affects cooling of the casting is the heat transfer coefficient between the casting and the mold. Still, as can be seen in Figure 3b, the predicted thermal profiles at TC1 and TC3 match well, demonstrating the validity of the chosen heat transfer coefficients. Any slight time delay discrepancy on fit for any given model-experiment thermocouple pair is attributed to the slight variability in contact time between the melt and the thermocouple and/or error in knowledge of the thermocouple location.

Table 2 shows that the tuned heat transfer coefficients for Trial C are approximately 10% larger than for Trials A, and B at temperatures where solidification is taking place. Correspondingly, Table 1 shows that the average cooling rate during solidification for Trial C was approximately 10% larger than for Trials A and B. We hypothesize that this difference is due to our inability to pour the liquid metal in an entirely repeatable fashion; with such a small casting, even slight variation in the initial location of melt/mold contact and trajectory of the pour has an impact on the rate of cooling, especially at high temperatures. Note however, that all three trials resulted in similar microstructure, as confirmed via measurements of secondary dendrite arm spacing (SDAS), which was found to be: $\lambda_{2,Trial\ A}$= 25.2μm, $\lambda_{2,Trial\ B}$= 23.1μm and $\lambda_{2,Trial\ C}$= 23.2μm. This small spacing is linked to the high cooling rate experienced during solidification (5-15 K/s) of each casting [8].

Due to the small size of the casting, ~ 200 g, the manner in which latent heat is evolved within the model plays a significant role in ensuring that the predictions match the experimental data. Further, for industrial alloys with a considerable fraction of eutectic, like A356, the temperature over which the non-equilibrium eutectic transformation occurs, and hence the latent heat evolves, is uncertain and highly variable as it depends on cooling conditions and local composition. Our initial simulations estimated the evolution in latent heat using a fraction solid / temperature curve based on a relationship found in the literature [4]. However, through the iterative process of tuning the heat transfer coefficients, it became clear that the thermal model could not be fit to the experimental data unless an improved evolution in fraction solid with temperature curve could be determined matching the experimental results.

To estimate the evolution of fraction solid versus temperature that occurred during the T-shaped casting experiments, the equation-based Newtonian (EBN) method of cooling curve analysis [7] by Gibbs and Mendez was applied. The results, based on the temperature measurements at TC2, are shown in Figure 4 for each experiment. As can be seen, the fraction solid versus temperature curves for Trials A and C are quite similar, while the curve for Trial B seems shifted. It is hypothesized that perhaps the melt in Trial B was poured in such a way that a coherent dendritic structure formed almost immediately along the bottom of the mold, accelerating the evolution in fraction solid. However, the thermal curves for Trials A and B were quite similar, and the transformation temperatures for all three trials all seem to agree with each other despite the shift in Trial B fraction solid. The observed delayed onset of the solidus temperature as compared to the phase diagram is in agreement with phenomena reported by Thompson [4]. The formation of Mg_2Si (not typically seen in near-equilibrium cooling conditions [12]) also appeared at temperatures consistent with those reported by Thompson at high cooling rates. The data from each curve was used for the individual casting simulations, to capture the observed variations in latent heat evolution. This cooling curve analysis is a key feature of the combined numerical/experimental method for determining solidification contraction coefficients in A356.

The measured displacements of the moving wall for all three trials are shown in Figure 5a. These values are negative because the contraction of the casting causes the wall to move into the mold. As can be seen, all three trials produced very similar results, demonstrating the robustness of the T-shaped casting mold for measuring solidification contractions. The values of the TCC parameter based on the experimental data, calculated using Eq. (1), are shown in Figure 5b as a function of temperature at TC2. This data provides significant insight into solidification contraction. First, it would appear that contraction initiates at a temperature where the non-equilibrium primary eutectic reaction begins to occur, at 841 K (568˚C) as was assumed in Section 2. Then, the rate of contraction varies significantly as the casting cools, increasing and decreasing at various temperatures. While some of the observed features will be linked to the fact that there is a temperature gradient along the longitudinal direction, the temperature corresponding to changes in behavior generally matches with the initiation of the primary eutectic reaction, the formation of Mg_2Si and the depressed solidus temperature. Note that the TCC parameter values reported in Figure 5b are not the same as a thermal strain coefficients, nor the coefficient of thermal contraction/expansion. The TCC parameter represents a change in casting length relative to the gauge length of the sample as a function of temperature, as noted in Equation 1. Thus, the TCC parameter is a measurement of the *integrated* dimensional change of the casting relative to a measured temperature at some point (in this case, TC2). This is different than a strain occurring at an infinitesimal point in the casting due to a thermal change at that same point, which is what the thermal strain coefficient represents. The values are in the same order of magnitude and are equivalent in unit due to the similar characteristics they represent. The value of the thermal strain coefficient for the high temperature, solid phase α for LM25 (Al-7Si-0.2Cu, $\alpha=2.6\cdot10^{-5}$ K^{-1}), reported by Mills [8] has been included in Figure 5b for comparison.

Using the experimentally-measured displacement data and corresponding TCC parameter values, an iterative process was applied to determine the thermal strain coefficients required to accurately model the displacement of the moving wall. Initially, the entries in the UEXPAN user-written subroutine of the Abaqus FE solver matched the TCC parameter data. The values were then modified to improve the fit of the predictions to the experimental displacement curves presented in Figure 5a. The final thermal strain coefficients used in all three stress simulations are reported in Table 4 as a function of temperature.

The model-predicted displacement of the moving wall as a function of time is also shown in Figure 5a. As can be seen, through parameter tuning, a very good match is achieved for Trials A and C. The fit for Trial B is weaker, especially at early times. This is related to the difference in fraction solid evolution as observed in Figure 4. The corresponding predicted TCC parameter values are given in Figure 5b. Here, there is generally good agreement between the experimental and simulated results, although some of the fine features are not captured. Most importantly, the predicted TCC parameter values vary significantly as the casting cools in the same manner as the measured TCC parameter values, both increasing and decreasing at similar temperatures.

The displacement measurements and predictions shown in Figure 5a can also be compared to the known solidification shrinkage value for the A356 alloy, 4.1% based on the density comparison (ρ_{liq}=2420 kg/m^3 and ρ_{sol}=2550 kg/m^3 [13]). If the assumption is made that the T-shaped casting only contracts on the open top face and the moving wall, the overall volumetric changes between the liquid and solid states using the displacement magnitudes recorded in Figure 5a is calculated to be approx. ~1.15%. The significant difference between this value and the known solidification shrinkage is thought to manifest through the slight gaps formed at casting mold interfaces and on the corners of the mold.

Conclusions

In this study, the solidification contraction of an aluminum A356 alloy has been measured using a combined numerical/experimental approach. This temperature-dependent material property, knowledge of which is critical for improving casting quality, is extracted by tuning the thermal strain coefficients within a thermal/stress simulation based on their similarity to the measured evolution in casting contraction. Key to this analysis is (1) the use of a T-shaped mold which ensures oriented contraction, and (2) cooling curve analysis to accurately represent the release of latent heat within the mathematical simulation. The measured thermal contraction coefficients can be used as part of process models to improve the predictions of thermal contraction during aluminum shape casting processes.

Acknowledgements

The authors gratefully acknowledge the assistance of C. Reilly, J. Kantharaju and S. Bhatia for their help in conducting the casting trials and developing the model, as well as E. Smith for constructive feedback on the manuscript text. This research was funded by the Natural Sciences and Engineering Research Council of Canada.

References

[1] J. Campbell: Castings, Butterworth-Heiniemann, Oxford, 1991.

[2] I.I. Novikov: Goryachelomkost tsvetnykh metallov i splavov (Hot Shortness of Nonferrous Metals and Alloys), Nauka, Moscow, 1966.

[3] D.G. Eskin, Suyinto, J.F. Mooney, L. Katgerman: *Metall Mater Trans A*, 2004, vol. 35A, pp. 1325-1335.

[4] S. Thompson. Effect of cooling Rate on Solidification Characteristics of Aluminum Alloys A356 and AA5182. MASc Thesis. The University of British Columbia, Vancouver, Canada, 2003.

[5] O. Elsebaie, A.M. Samuel, F.H. Samuel: *J Mater Sci*, 2011, vol. 46, pp. 3027-3045.

[6] B. Zhang, D.M. Maijer, S.L. Cockcroft: *Mater Sci Eng A*, 2007, vol. 464, pp. 295-305.

[7] J.W. Gibbs, P.F. Mendez: *Scripta Mater*, 2008, vol. 58, pp. 699-702.

[8] K.C. Mills: Recommended Values of Thermophysical Properties for Selected Commercial Alloys, Woodhead Publishing Ltd, Cambridge, England, 2002, pp. 43-49.

[9] H.J. Frost, M.F. Ashby. Deformation-Mechanism Maps: The Plasticity and Creep of Metals and Ceramics, Pergamon Press, Oxford, 1982.

[10] M.J Roy, D.M. Maijer: Light Metals 2012, ed. C.E. Suarez, John Wiley & Sons Inc., Hoboken, NJ, USA. 2012, pp. 377-382.

[11] H. Hao, D.M. Maijer, M.A. Wells, A. Phillion, S.L. Cockcroft: *Metall Mater Trans A*, 2010, vol. 41A, pp. 2067-2077.

[12] H.B. Dong, M.R.M. Shin, E.C. Kurum, H. Cama, J.D. Hunt: *Metall Mater Trans A*, 2003, vol. 34A, pp. 441-447.

[13] S. Thermalingam, C.H. Caceres, J.A. Taylor: *Metall Mater Trans A*, 2013, vol. 44A, pp. 4071-4080.

Figures and Tables

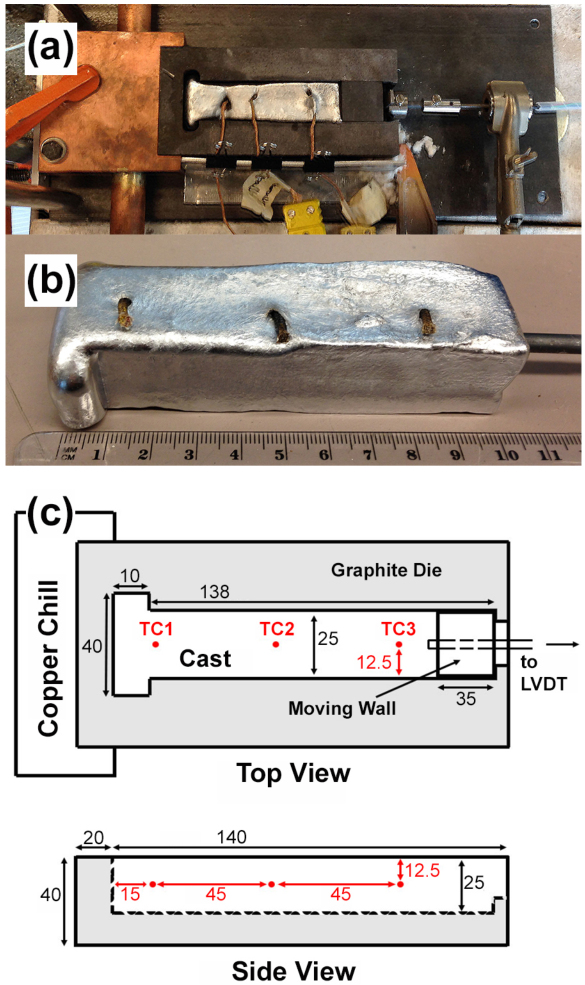

Figure 1 (a) Experimental setup of graphite mold, copper chill, LDVT and T-shaped casting, (b) T-shaped casting with Invar rod and cast-in thermocouples, (c) schematic with mold dimensions and thermocouple locations.

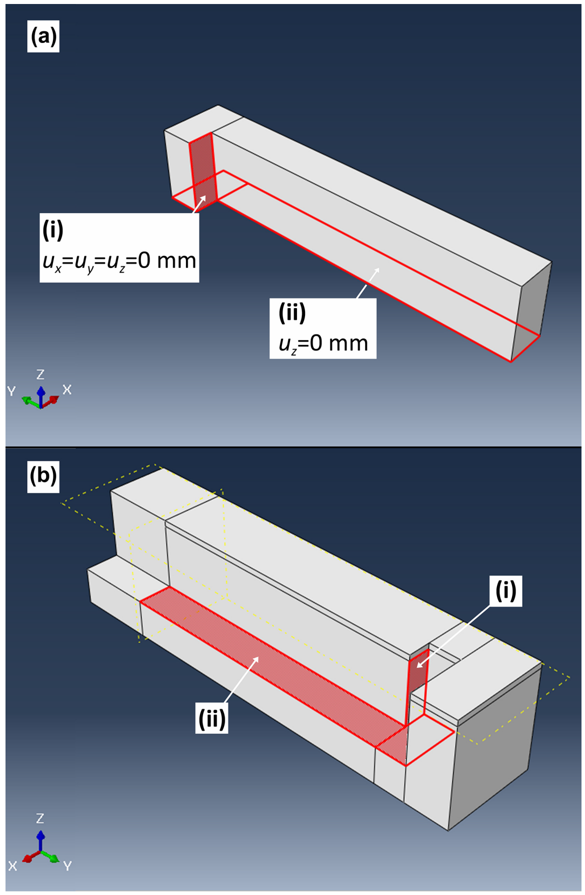

Figure 2 (a) Model of cast ingot showing the mechanical constraints; (b) Model of the graphite die, rotated 180 degrees about the z-axis, with corresponding constraint surfaces labelled.

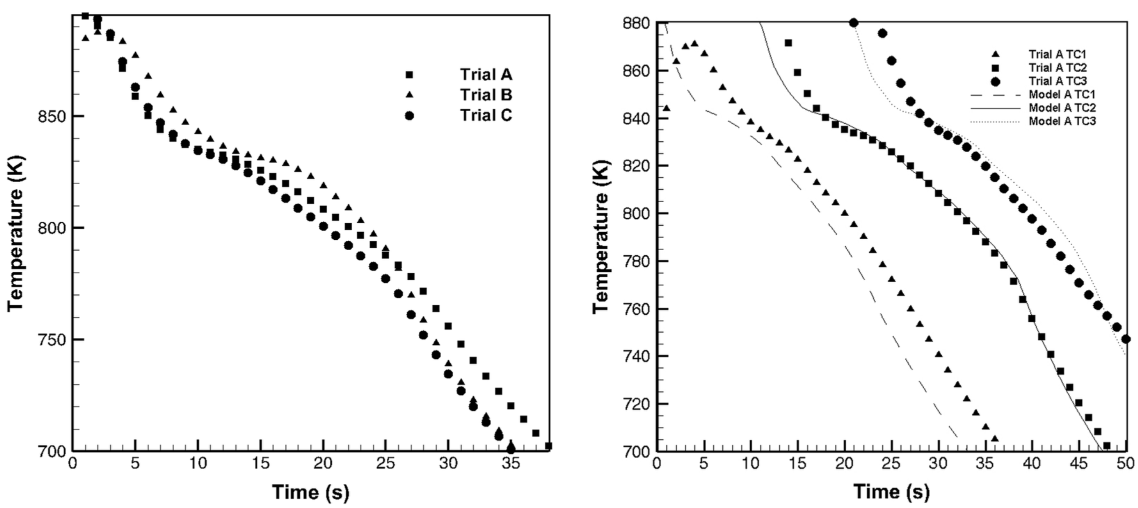

Figure 3 (a) Experimentally-measured time-temperature curves at TC2 for Trials A, B, and C; (b) experimental versus model temperature curves for trial A. In (b), the experimental data is shifted by 10s to more clearly show the comparison.

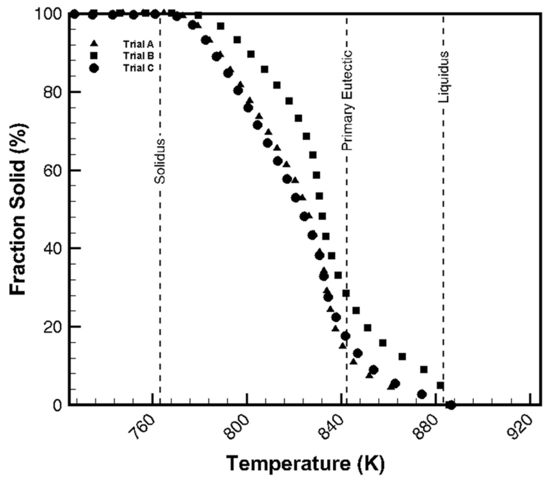

Figure 4 Evolution in fraction solid with temperature as modelled by the EBN method.

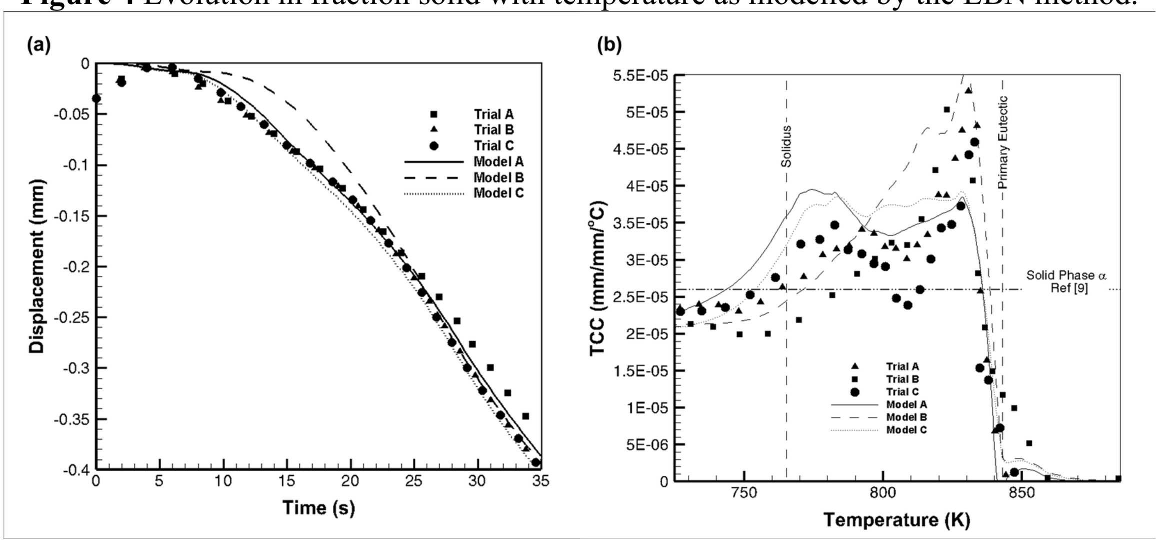

Figure 5 (a) Displacement during contraction (b) TCC parameter as calculated using the central thermocouple, TC2.

Table 1: Average cooling rates during solidification observed in experiments

Temp	(K/s)		
	Trial A	Trial B	Trial C
883-763 K (613-490 ˚C)	4.8	4.8	5.3

Table 2: Heat Transfer Coefficients used in the Thermal Model of the T-shaped casting

Interface	HTC (W/m²K)
Casting/Air & Mould /Air	50
Mould/Support Table	500
Mould/Copper chill	3000
Casting/Moving Wall	600
Casting/Mould	Discussed below

Table 3: Heat transfer coefficients for the casting / mould interface.

Temp	HTC (W/m²·K)		
	Trial A	Trial B	Trial C
923 K (650˚C)	2300	2300	2300
873-778 K (600-505 ˚C)	965	940	1045
763-713 K (490-440 ˚C)	400	420	450
698 K (425 ˚C)	350	350	350

Table 4: Thermal strain coefficients (including solidification contraction coefficients) used in the modelling of thermal contraction during solidification of Sr modified A356.

Temp	(mm/mm·K)
841 K (568 ˚C)	0.1
823 K (550 ˚C)	4.0
806 K (533 ˚C)	2.7
763 K (490 ˚C)	3.2
753 K (480 ˚C)	2.5